

## ATTENUATION LAWS FOR GALAXIES WITH DIFFERENT STAR FORMATION HISTORIES, BASED ON THE SDSS IMAGES

O. Vince

*Astronomical Observatory, Volgina 7, 11060 Belgrade 38, Serbia*

E-mail: *ovince@aob.bg.ac.yu*

(Received: January 13, 2009; Accepted: February 20, 2009)

**SUMMARY:** Attenuation curves (laws) in the optical part of the spectrum (from about 3500 Å to 9000 Å) are determined for galaxies with different star formation histories (SFHs) using images in five photometrical bands from the Sloan Digital Sky Survey (SDSS). Owing to large surveys like SDSS, it is possible to define several subgroups of galaxies with similar SFHs using two spectral indices that trace SFH. Attenuation curves are analyzed in terms of SFH and compared to the curves that are often used for dust correction of the observed data.

**Key words.** Galaxies: photometry – Galaxies: ISM – Galaxies: stellar content

### 1. INTRODUCTION

Young starburst galaxies are very dusty and the dust makes interpretation of their intrinsic physical properties very difficult. Beside dimming, the dust changes their spectra/color in a similar way as metallicity and age do (dust-age-metallicity degeneracy). Galaxies with old stellar population or with higher metal content or with more dust all are made redder to our instruments. To be able to interpret their intrinsic properties, this degeneracy must be broken first, and the dust properties are to be determined later if one wants to correct for the dust effect. This task turned out not to be so easy to accomplish and many researchers still making efforts to solve this problem.

The usual way to correct for the dust effect is to use the extinction curves of the Milky Way (MW), Small Magellanic Cloud (SMC) or Large Magellanic Cloud (LMC). Since stars in these galaxies can be resolved, the most straightforward way do determine their extinction law is to observe similar stars with different dust content and to normalize their spectra

(more obscured with dust-free; pair method). An effective extinction curve for the whole galaxy is then calculated as average of these curves. There are several problems when we use these curves for dust correction for all (even distant) galaxies: although these three galaxies are physically different they do not cover the whole range of galactic types that exist in the Universe. Furthermore, dust obscuration of stars is physically different process with respect to dust obscuration of distant galaxies. In the former case, dust obscuration is called extinction. It can be simply modeled as a screen of dust in front of point-source and is easily studied by solving a radiative-transfer problem in the layer of dust and gas. For distant galaxies the obscuration is far more complicated physical process. It depends on the geometrical properties of stars versus dust and optical/physical properties of dust in the same time. Obscuration in this case is called attenuation.

Calzetti et al. (1994) applied pair-method to determine attenuation curve for a UV selected sample of starburst galaxies. Using 39 carefully selected galaxies, they divided them into bins of dust indicator (attenuation bins). The averaged spectra in the

bins were normalized with the least attenuated one (dust-free) and the obtained curves were averaged to get the effective attenuation law for this sample. Beside MW, SMC and LMC extinction laws, Calzetti's law is very often used to correct galaxy spectra for the dust effect. A legitimate question is "is the Calzetti's law generally applicable to all types of galaxies?". We deal partially with this question in the recent work.

This work is a generalization of Calzetti's method. Owing to SDSS sky survey we deal with a large amount of photometric/spectroscopic data. Using spectral indices developed by Wild et al. (2007), galaxies are divided into bins (called boxes hereafter) where the dust-metallicity-age degeneracy is broken and the dust effect can be studied. Attenuation curves are determined in boxes and analyzed.

In the first section, the sample of starburst galaxies is described. In the second one, sub-samples of galaxies with similar SFH are defined. The method and the results are presented in the subsequent sections. In the last one we draw our conclusion.

## 2. THE SAMPLE

The data used in this work were taken from the Sloan Digital Sky Survey (SDSS) database. It is a large imaging and spectroscopic survey with an aim of obtaining data across  $\pi$  sr of the high Galactic latitude sky. Imaging is performed in 5 photometrical bands (u, g, r, i, z) with a drift-scan camera mounted on the 2.5m telescope at the Apache Point Observatory, New Mexico, USA (Fukugita et al. 1996, Gunn et al. 1998). Simultaneously, using two other telescopes, airmass, extinction coefficient and other relevant parameters were measured/determined in order to get accurate photometry of about 300 millions of celestial objects (galaxies, stars, quasars, planets and even asteroids). Spectra, on the other hand, were obtained using 3" fibers, positioned as close as possible to the centers of the target galaxies and covering a spectral range from 3800 to 9200 Å with resolution of about 1800. More details about the SDSS project, instruments and data (spectroscopic and photometric) can be found on <http://www.sdss.org/dr7/> or <http://cas.sdss.org/astrodr7/en/>.

In this work, five photometrical bands (u, g, r, i, z) are used to determine attenuation laws for galaxies with different. I use the same sample in this work as the one defined to determine attenuation laws from galaxy spectra (Vince et al. 2009). In brief, it was defined using 6<sup>th</sup> data release (DR6) of the SDSS database with the following selection criteria:

- (i) galaxies without active galactic nuclei (AGN) in the center of the galaxies were selected using Baldwin, Phillips and Terlevich diagram (BPT - diagram; Baldwin et al. 1981),
- (ii) extremely inclined galaxies with axial ratio  $< 0.4$  were excluded,

- (iii) only the high signal-to-noise (S/N) spectra with median S/N  $> 10$  in the g-band were taken,
- (iv) S/N in the strong emission lines used for BPT diagram were required to be greater than 5 and
- (v) galaxies with the redshift between 0.05 and 0.25 were taken.

More details about the selection criteria can be found in Vince et al. (2009). We end up with about 100 000 galaxies with these criteria applied.

The motivation to use photometric data to determine the attenuation curves is twofold: 1. spectra are obtained through 3" fiber and for the large number of galaxies only their central part is observed, and 2. comparing results with the ones obtained from the spectra, we may learn about aperture biases. Furthermore, UV and IR photometric data can be found in larger number in databases (GALEX, Spitzer, 2MASS and so on) than spectra and the sample can be more easily matched and extended into these parts of the spectrum. Extension into UV is of great importance because the effect of dust is the biggest in this part of the spectrum. IR wing on the other hand is important when absolute calibration is needed because the dust effect can be neglected there. Furthermore, as the photometric data are more numerous, the statistical analysis can be more accurate.

## 3. THE SUB-SAMPLE OF GALAXIES WITH SIMILAR SFH

Before extracting the galaxies with similar SFHs, they were divided into two metallicity groups: low metallicity group with gas metallicity lower than solar ( $\log(\text{O}/\text{H})+12 < 8.9$ ), and higher than solar ( $\log(\text{O}/\text{H})+12 > 8.9$ ). In this way, the dust-metallicity degeneracy is broken. Gas metallicities were determined by Tremonty et al. (2004) and can be found in the MPA/JHU database (<http://www.mpa-garching.mpg.de/SDSS/DR4/>).

Galaxies with similar SFHs were defined using the first two principal components (PC) of the principal component analysis (PCA) performed on the galaxy spectra with narrow spectral range around 4000 Å-break. As shown by Wild et al. (2007), PC1 correlates well with 4000 Å-break and PC2 correlates with the excess of  $H\delta_A$  index (see Worthey et al. 1994, and Worthey and Ottaviani 1997, for definitions of the 4000 Å-break and  $H\delta_A$  indices). These two indices on the other hand are good tracers of SFH (Kauffmann et al. 2003). See also Wild et al. (2007) for more details about PC1 and PC2.

The two metallicity groups are divided into 11 PC1-PC2 sub-samples (which will be called 'boxes' hereafter). Fig. 1 shows galaxies in the PC1-PC2 space and boxes that enclose galaxies with similar SFH (red squares). Boxes were chosen to be small enough to contain only galaxies with similar spectral shape (similar SFH) and sufficiently large to contain

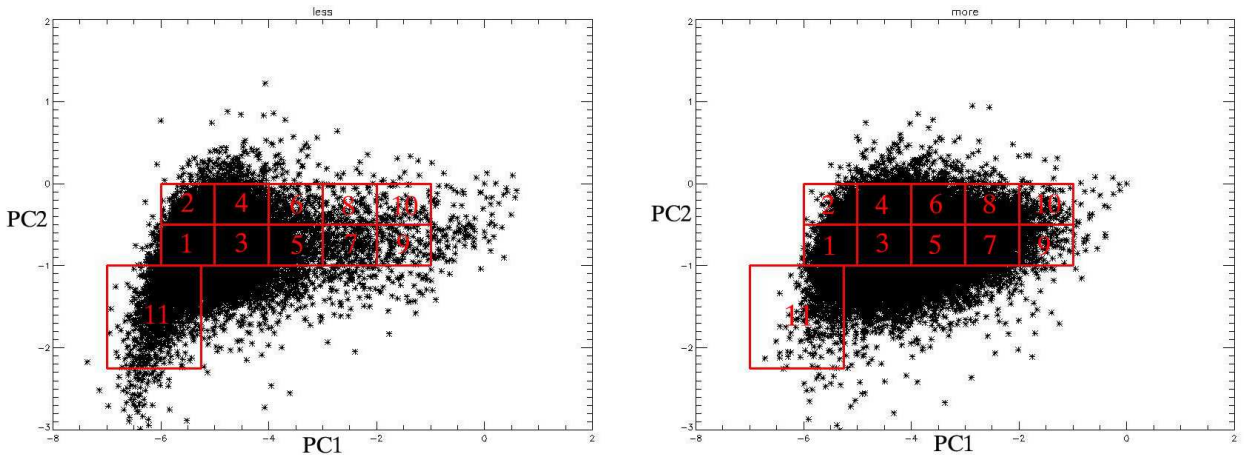


**Fig. 1.** Galaxies in the PC1-PC2 space for low and high metallicity groups on the left and right panels respectively. ‘Boxes’ are defined as illustrated with red squares and designated with numbers as indicated on both panels.

enough galaxies for statistical analysis. Boxes cover starburst galaxies (boxes 1 and 2), star-forming galaxies (boxes 3-5) and green-valley galaxies (boxes 7-10). Box 11 contains the youngest galaxies in the sample. Galaxies with  $PC2 > 0$  are post-starburst galaxies and for these galaxies boxes were not defined (see Vince et al. (2009) for more details about the definitions of these types of galaxies).

#### 4. THE METHOD

Each box was divided into 10 bins using the dust indicator defined by Calzetti et al (1994):

$$\tau_B^l = \tau_\alpha^l - \tau_\beta^l = \ln\left(\frac{H_\alpha/H_\beta}{2.86}\right) \quad (1)$$

where  $H_\alpha/H_\beta$  is the Balmer line ratio,  $\tau_\alpha^l$  and  $\tau_\beta^l$  are optical depths in the Balmer emission lines, 2.86 is the theoretical value expected for unreddened  $H_\alpha/H_\beta$  ratio taken from Osterbrock (1989) and superscript l indicates that  $\tau_B^l$  is obtained from the emission lines.

Attenuation bins,  $\tau_B^l$ , were divided from 0 to 1 with step 0.1. Only the first six attenuation bins were used in the following because other bins are too poorly populated by galaxies to perform the statistical analysis. Number of galaxies in the boxes and corresponding attenuation bins for both metallicity groups are shown in Table 1. In ‘total’ columns, the total number of galaxies in the boxes can be found.

As mentioned above, magnitudes obtained in 5 optical bands (u, g, r, i, z) are used to determine the attenuation curves for galaxies in boxes. The Petrosian magnitudes are used in this work (see <http://www.sdss.org/dr7/algorithms> for definition of the Petrosian magnitudes). They are stored

in the SDSS database as petroMag. They are defined to be independent of the position and distance of the galaxy (Petrosian 1976). The Petrosian magnitudes (as well as all other magnitudes in the SDSS database) are expressed in asinh magnitudes, i.e. luminosities (Lupton et al. 1999) according to:

$$m = -\frac{2.5}{\ln(10)} * [a \sinh\left(\frac{f/f_0}{2b}\right) + \ln(b)], \quad (2)$$

where  $f/f_0$  is the ratio of the observed count rate to the zero-point count rate and b is the softening parameter which is tabulated for each of the five photometric bands (see <http://www.sdss.org/dr7/algorithms/index.html> for more details). Since the SDSS system is intended to be AB system (by which a magnitude 0 object should have the same counts as a source of  $F = 3631$  Jy), conversion to flux density is given by  $S = 3631 * f/f_0 [Jy]$  (there are small offsets in photometric zero-points for u and z bands described at the Web link given above).

The steps in the method are same for all boxes and will be described using Fig. 2. (this figure corresponds to the box 1 of the low metallicity group)

1. First, the fluxes in the attenuation bins are averaged (panel a).

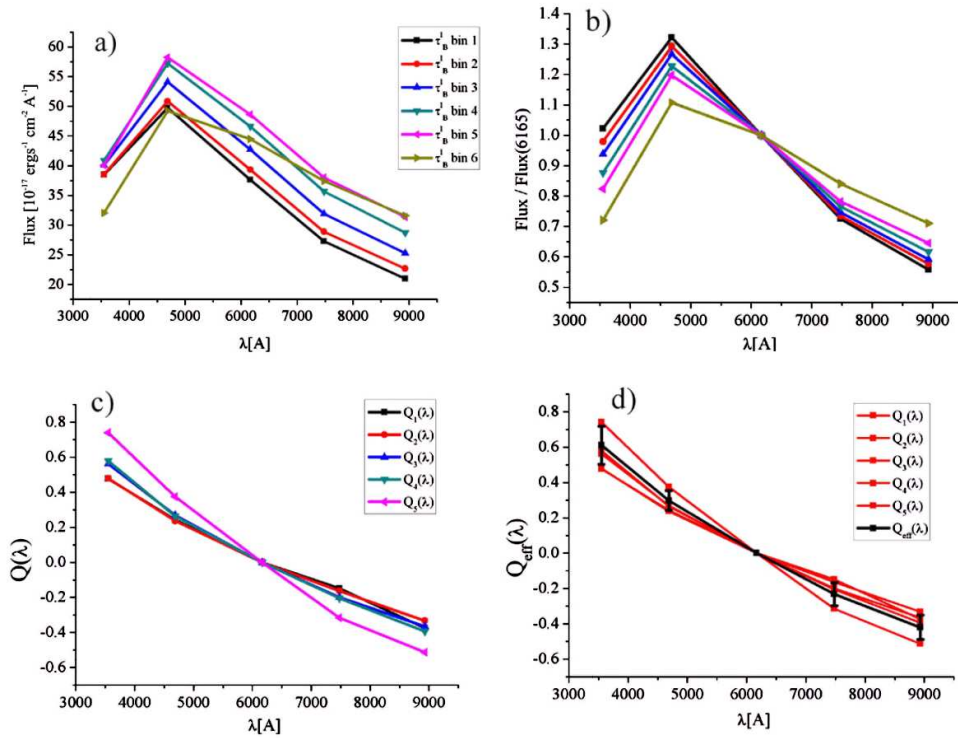
2. The fluxes are then normalized in the r-band i.e. 6165 Å. Since galaxies are divided into two metallicity groups and into 11 sub-groups where galaxies have similar SFH, we expect that the age-dust-metallicity degeneracy is broken. Thus, any change in the shape of these curves can be attributed to the dust effect (panel b).

3. The attenuation curves are calculated according to:

$$Q_n(\lambda) = \frac{\tau_n(\lambda)}{\delta\tau_{Bn}^l} \quad (3)$$

**Table 1.** Number of galaxies in the boxes and corresponding first 6 attenuation bins that are used in this study. See text for details.

low metallicity group								high metallicity group							
$box/\tau_B^l$	1	2	3	4	5	6	<i>total</i>		1	2	3	4	5	6	<i>total</i>
1	651	1766	1488	411	71	15	4404		8	219	1032	1275	705	260	3584
2	161	482	473	209	44	11	1384		1	33	203	310	189	87	867
3	364	1197	1275	534	132	22	3530		52	694	2983	4666	3473	1691	4311
4	155	505	609	355	112	32	1785		16	201	811	1488	1377	812	5297
5	65	163	170	107	41	19	577		86	574	1871	2808	2381	1255	9804
6	26	56	69	57	24	19	261		42	175	545	851	912	662	3922
7	38	65	46	27	13	10	203		98	323	661	871	716	362	3272
8	14	20	23	23	12	3	98		51	167	309	385	337	198	1685
9	35	13	18	7	2	4	79		25	39	99	98	67	43	390
10	12	15	16	5	4	2	55		21	36	60	77	71	38	334
11	626	1180	648	149	24	7	2634		11	129	471	409	146	46	1227


**Fig. 2.** The steps of the method of determination of the attenuation curves. See text for details.

where  $n = 1, 2, 3, 4, 5, 6$ , counts attenuation bins,  $\tau_n(\lambda)$  is the natural logarithm of the normalized spectra, i.e.

$$\tau_n(\lambda) = -\ln\left(\frac{F_n(\lambda)}{F_1(\lambda)}\right), \quad (4)$$

and

$$\delta\tau_{Bn}^l = \tau_{Bn}^l - \tau_{B1}^l. \quad (5)$$

Balmer optical depths,  $\tau_B^l$ , in Eq. (5) are calculated using Eq. (1). The attenuation curves are shown in panel c.

4. The effective attenuation curve,  $Q_{\text{eff}}(\lambda)$ , for the whole box is calculated as the weighted average (weighed by  $\delta\tau_{Bn}^l = \tau_{Bn}^l - \tau_{B1}^l$ ) of the 5 attenuation curves from the previous panel.  $Q_{\text{eff}}(\lambda)$  is illustrated in panel d with the black curve.  $Q_n$ s from the previous panel are shown in red for comparison. Error bars are a combination of formal errors (error of the mean of the Petrosian fluxes in the attenuation bins propagated by the bootstrap method) and dispersion of  $Q_n$ s. Since the photometry is quite good (uncertainty less than 1%) and there are quite a lot of galaxies in the attenuation bins, error of the mean

is small and their contribution to the error bars is small.

5. Finally, the effective attenuation curve is fitted with the natural logarithm of the power law i.e.  $\ln(A(\lambda) - S)$ .  $S$  is taken as a measure of the slope of the  $Q_{\text{eff}}(\lambda)$  and is used in the analysis.

Calzetti et al. (1994) fitted their attenuation curve with polynomial function of the 3<sup>rd</sup> degree. They fit the attenuation curve in broader spectral range (1250-8000 Å) and polynomial function proved to be a good choice for fitting. We derived attenuation curves from 3500 to 9000 Å and in this spectral range logarithm of the power law is as good fitting function as polynomial function of the 3<sup>rd</sup> degree. Since we would like to compare the attenuation curves for galaxies with different SFH and since  $S$  in the  $\ln(A(\lambda) - S)$  uniquely describes their slopes, we have chosen this function to fit the curves.

## 5. THE RESULTS

The coefficients of the power law fitted to the attenuation curves in boxes ( $A$ ,  $S$ ) and standard deviations of the estimate are shown in Table 2. According to the fourth column,  $\ln(A(\lambda) - S)$  is a good choice to fit the attenuation curves in the optical part of the spectrum.

The effective attenuation curves for the low metallicity group are plotted in Fig. 3. Curves in the boxes are designated with different colors as shown in the legend. For comparison, curve of the first box with error bars is superimposed in bold orange. Since these error bars are typical for both metallicity groups, other error bars are not plotted on the graph. Error bars are quite large but not larger than the dispersion of the effective attenuation curves themselves.

In bold magenta curve, the Calzetti's law is superimposed. As can be seen, attenuation curves determined in this work are all shallower than the Calzetti's one which is closest to the box 11, i.e. to the youngest galaxies. This was to be expected since Calzetti's sample are UV-selected galaxies that are

young and dusty. The extinction curves of the Milky Way, Small Magellanic Cloud and Large Magellanic Cloud are even steeper than the Calzetti's law and were not plotted on this graph (see Fig. 1. of Calzetti et al. (1994)).

**Table 2.** The coefficients of the fitting functions ( $\ln(A)$ ,  $S$ ) of the attenuation curves and their standard deviations.

box num.	$\ln(A)$	$S$	std dev
1	9.77647	1.12114	6.78E-03
2	9.05703	1.04021	2.75E-02
3	8.49822	0.97335	2.14E-02
4	8.44827	0.96878	2.31E-02
5	6.30196	0.72418	2.60E-02
6	5.88947	0.67152	6.56E-02
7	1.68623	0.19109	2.67E-02
8	3.78606	0.42854	0.13
9	4.00839	0.46304	0.10
10	1.89915	0.22228	6.86E-02
11	12.33333	1.41658	5.33E-02

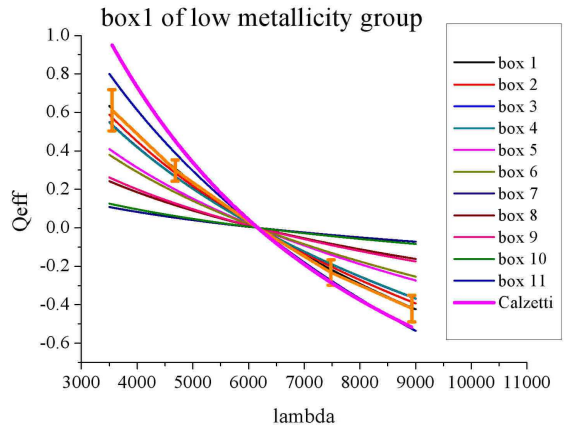


**Fig. 3.** All 11 attenuation curves for the low metallicity group are shown. See text for details.

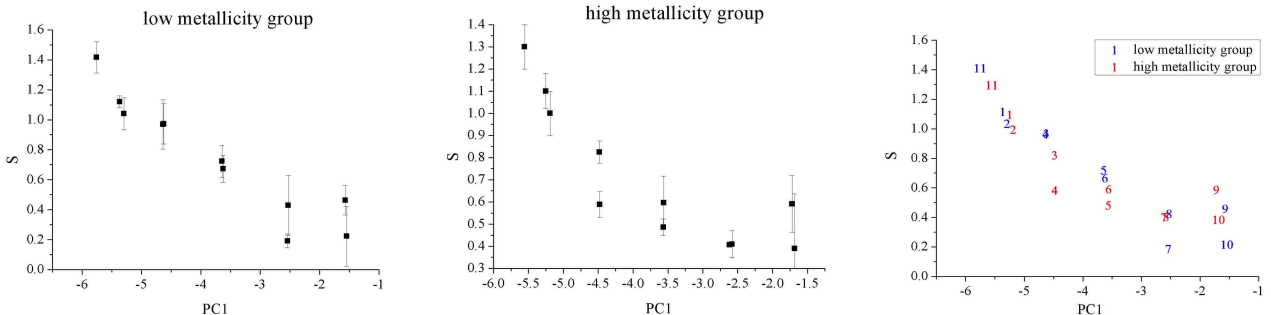


**Fig. 4.** Slope  $S$  versus  $PC1$  for low (left) and high (middle) metallicity groups respectively. The same trend for both metallicity groups is presented in the right panel. The numbers are the box numbers.

Fig. 4 shows  $S$  versus average PC1 in the corresponding boxes for the low metallicity group (left panel) and high metallicity group (middle panel) respectively. As can be seen, there is a trend of  $S$  with respect to PC1 for both groups i.e. more quiescent galaxies (larger PC1) are on the average less dusty and the slope of the attenuation curve is smaller. Panel on the right shows the same dependence with both metallicity groups with points designated by box numbers. As can be seen, both metallicity groups follow the same trend and show no systematic difference between them.

## 6. CONCLUSION

The attenuation curves were determined for galaxies with different SFHs (defined by PC1 and PC2) using optical photometric data from the SDSS database. To break the dust-metallicity degeneracy, the sample was first divided into 2 distinct metallicity groups. Then the sample was divided into 11 PC1-PC2 sub-groups containing galaxies of similar SFH. Method applied by Calzetti (1994) was used to determine the attenuation curves. They were fitted with logarithm of the power law, which enables us to interpret the attenuation curves in terms of their slope ( $S$ ) and compare the curves among themselves. The slope of the attenuation curves shows the trend with PC1 in the sense that more active starburst galaxies are dustier. Curves were compared with the Calzetti's law, showing that the Calzetti's curve match only with attenuation curve of the youngest galaxies in the sample. Using the Calzetti's attenuation law for all galaxies would thus erroneously correct for the dust effect. The same holds for the extinction curves of MW, SMC and LMC are applied for dust correction since these curves are even steeper than the Calzetti's law.

*Acknowledgements* – This work was supported by the Ministry of Science and Technological Development of the Republic of Serbia through the project no. 146012, "Gaseous and stellar component of galaxies: interaction and evolution".

## REFERENCES

- Baldwin, J. A., Phillips, M. M., Terlevich, R.: 1981, *Publ. Astron. Soc. Pacific*, **93**, 5B.
- Calzetti, D., Kinney, A. L., Storchi-Bergmann, T.: 1994, *Astrophys. J.*, **429**, 582.
- Fukugita, M., Ichikawa, T., Gunn, J. E., Doi, M., Shimasaku, K., Schneider, D. P.: 1996, *Astron. J.*, **111**, 1748.
- Gunn, J. E., Carr, M., Rockosi, C., Sekiguchi, M., Berry, K., Elms, B., de Haas, E., Ivezić, Z., Knapp, G., Lupton, R. et al.: 1998, *Astron. J.*, **116**, 3040.
- Kauffmann, G., Heckman, T. M., White, S. D. M., Charlot, S., Tremonti, C., et al.: 2003, *Mon. Not. R. Astron. Soc.*, **341**, 33.
- Lupton, Robert H., Gunn, James E., Szalay, Alexander, S.: 1999, *Astron. J.*, **118**, 1406.
- Osterbrock, D. E.: 1989, *Astrophysics of Gaseous Nebulae and Active Galactic Nuclei*. Univ, Sci. Books, New York.
- Petrosian, V.: 1976, *Astrophys. J.*, **209**, L1.
- Tremonti, C. A., Heckman, T. M., Kauffmann, G., Brinchmann, J., Charlot, S. et al.: 2004, *Astrophys. J.*, **613**, 898.
- Vince, O., et al.: 2009, in preparation.
- Wild, V., Kauffmann, G., Heckman, T., Charlot, S., Lemson, G., Brinchmann, J., Reichard, T., Pasquali, A.: 2007, *Mon. Not. R. Astron. Soc.*, **381**, 543.
- Worthey, G., Faber, S. M., Gonzalez, J. J., Burstein, D.: 1994, *Astrophys. J. Suppl. Series*, **94**, 687.
- Worthey, G. and Ottaviani, : 1997, *Astrophys. J. Suppl. Series*, **111**, 377.

**ОДРЕЂИВАЊЕ ЗАКОНА СЛАБЉЕЊА ЗРАЧЕЊА ЗВЕЗДА У  
ГАЛАКСИЈАМА РАЗЛИЧИТИХ ИСТОРИЈА ФОРМИРАЊА  
ЗВЕЗДА НА ОСНОВУ SDSS ФОТОМЕТРИЈСКИХ ПОСМАТРАЊА**

**O. Vince**

*Astronomical Observatory, Volgina 7, 11060 Belgrade 38, Serbia*

E-mail: *ovince@aob.bg.ac.yu*

УДК 524.7 – 472

*Оригинални научни рад*

У овом раду одређени су закони слабљења зрачења звезда у галаксијама услед дејства прашине (attenuation laws) користећи 5 фотометријских података из базе Sloan Digital Sky Survey (SDSS). Захваљујући великом броју података у бази и користећи два спектрална индекса који једнозначно одређују ис-

торије формирања звезда (Star Formation History; SFH), дефинисане су подгрупе галаксија са сличним SFH и одређени су им закони слабљења. Ови су затим анализирани и упоређени са законима који се често користе у литератури.